Journal Name

ARTICLE

MOF – cation exchange resin composites and their use for water decontamination

Received 00th January 20xx,
Accepted 00th January 20xx

DOI: 10.1039/x0xx00000x

www.rsc.org/

Ping He,[a] Kok-Giap Haw,[a] Jiawang Ren,[a] Qianrong Fang,[a] Shilun Qiu,[a] Valentin Valtchev[a,b*]

Macroporous cation exchange resin beads were subjected to hydrothermal treatment in a ZIF-8 yielding solution resulting in a resin beads – MOF composite. The resin beads were employed as a shape providing carrier and support for the growth of MOF crystals. The conditions of synthesis were optimized so as to obtain maximum MOF loading. The final composites and their intermediates were characterized with complementary physicochemical methods, including XRD, SEM, thermal analysis (TG) and nitrogen sorption. The obtained composites were employed for water decontamination targeting a dye (methyl blue) and a medical (antibiotic) contaminant. The composite adsorbent showed excellent removing ability in recyclability, which exceeds the performance of building components, i.e., cation exchange beads and pure ZIF-8 material.

Introduction

Nowadays with the rapid development of industry and the growth of population, unwanted products or by-products of human activities are discharged in water systems, which bring health problems for plants, animals, and human being.[1] Various organic compounds that are toxic, recalcitrant, mutagenic and carcinogenic are disposed without any treatment.[2-3] Among the countless contaminations, dyes and antibiotics, which are extremely largely used in different industries and hard-biodegradable, present serious environmental problem.

Large variety of wastewater treatment methods are available, including chemical oxidation, membrane separation, chemical coagulation/flocculation, biosorption, electrochemical treatment, selective adsorption, etc.[4-7] Among these methods the selective adsorption offers the advantages of low cost, low energy consumption and simple operation. Adsorptive removal processes are based on the use of porous solids such as zeolites, clays and activated carbon.[8-9] Each of these materials offers certain advantages and the selection of the material for a particular separation/depollution depends on a number of factors, including the ability of the material to be engineered. Zeolite molecular sieves are largely used in water depollution because of their high stability, reasonable price and already developed shaping technology.[10] On the other hand, the pores of industrial relevant zeolites are limited to 7.3 Å in size, which makes these materials hardly applicable when large organic pollutants are targeted.[10]

Metal–organic frameworks (MOFs) is a relatively new class of crystalline porous solids built up of metal nodes and organic ligands.[11] Certain MOF materials offer substantial larger pores and higher micropore volume than the conventional zeolite crystals. Owing to their features as unsaturated metal sites, modifiable pores, and ultra-high specific surface area, MOF materials show promising performance in various applications including adsorption, separation, catalysis and chemical sensing.[12–14] MOF molecular sieves offer also great opportunities of pollution abatement, including water decontamination. However, the route to their practical uses is passing through the preparation of properly shaped bodies for ease of handling and recyclability.[15-19]

Different methods of MOF shaping were reported. Aguado et al. grew in situ SIM-1 films on millimeter-sized alumina supports.[20] O'Neill et al. deposited crystalline MOFs into mm-sized macro-porous polyacrylamide carrier.[21] Bui et al. immobilized ZIF crystals on the surface of macro-porous phyllosilicate mineral using the sequential addition of precursors.[22] Abbasi et al. used polyether sulfone as a binder to fabricate MOF beads.[23] The preparation of shaped MOF bodies and foams by applying carboxymethylcellulose as a binder was also reported.[24] Each of these methods offer advantages and disadvantages, however no general approach that could be applied to any MOF material is available to date.

Our approach is based on the use of macroporous cation exchange beads, which is a carrier and shaping template. The macroporous beads exhibit large macropore space where ZIF-8 crystals can be deposited by in situ growth.[25-27] Besides a carrier, the ion exchange bead is expected to be an active component that immobilizes positively charged species. Methyl blue (MB) and oxytetracycline (OTC) were used to test the decontamination ability of the composite. MB is an anionic dye and a drug widely used as biological stain, while the OTC belongs to tetracycline broad-

[a] State Key Laboratory of Inorganic Synthesis and Preparative Chemistry, Jilin University, Changchun 130012, China.
[b] Normandie Univ, ENSICAEN, UNICAEN, CNRS, Laboratoire Catalyse et Spectrochimie, 6 Marechal Juin, 14050 Caen, France.
Email : valentin.valtchev@ensicaen.fr
Electronic Supplementary Information (ESI) available: [details of any supplementary information available]. See DOI: 10.1039/x0xx00000x

spectrum antibiotics, which is intensively used in human and animal treatments as antibacterial agents and growth factors.[28,29]

The objective of present study is to develop simple and versatile approach for shaping different MOF materials. The method is exemplified by the synthesis of ZIF-8 on macroporous cation exchange resin beads. A dye (MB) and an antibiotic (OTC) molecule are used as model contaminants and the ability of composite beads to decontaminate water is studied.

Experimental

Reactants

Zinc nitrate hexahydrate (Sigma-Aldrich, 98%), 2-Methylimidazole (Aladdin, 99%), Zinc chloride (TCI, >98.0%), Sodium formate (Sigma-Aldrich, >99.0%), Cobalt nitrate hexahydrate (Strem Chemicals, 99.0%), Methyl blue (J&K chemicals, 99%), L-Ascorbic acid (J&K chemicals, 99%), Oxytetracycline dihydrate (Aladdin, 99%), Methanol (Xilong scientific, >99.5%), Potassium bromide (Damao, 99.0%) and N, N-dimethylformamide (DMF, Sinopharm, >99.5%) were used in this study. All reagents were obtained from commercial sources and used without further purification. Deionized (DI) water was produced by a Milli-Q integral ultrapure water system and used in all experiments.

Composite material preparation

Macroporous cation exchange resin beads (Dowex 88, Na-form) were employed in this study. 1 g beads were immersed in 80 mL $Zn(NO_3)_2 \cdot 6H_2O$ solution for 6 h. The concentration of the solution was 0.5 M, 1.0 M and 1.5 M. The Zn-exchanged beads were separated by suction filtration, rinse with water and dried at 60 °C overnight. Two synthesis medium, water and methanol, were employed:

Method A: zinc nitrate hexahydrate (372 mg, 1.25 mmol) was dissolved in 5 mL deionized (DI) water and then 1.0 g zinc exchanged resin beads were added to the solution. 2-methylimidazole (4.105 g, 50 mmol) was dissolved in 45 mL DI water and added to the beads containing solution. The synthesis of ZIF-8 resin beads composite was carried out in a flask submerged in an oil bath at 60 °C for 1 day. MOF beads were separated by decanting of the supernatant, dispersed in methanol and treated in ultrasonic bath for 5 min to remove the loosely attached crystals. The procedure was repeated three times. The composite beads were dried at 60 °C overnight. ZIF-8 resin composite synthesized in water is denoted ZB-W-x, where the x is the concentration in mole of $Zn(NO_3)_2 \cdot 6H_2O$ solution used for Zn-exchange of initial resin beads.

Method B: zinc chloride (303 mg, 2.22 mmol), 2-methylimidazole (365 mg, 4.44 mmol) and sodium formate (303 mg, 4.46 mmol) were dissolved in methanol (30 mL) and stirred at room temperature for 1 h. This solution and 0.5 g Zn-exchanged resin beads were transferred to a Teflon-lined autoclave (50 mL). The synthesis of ZIF-8 resin composite material was performed in a tumbling oven (50 rpm) at 130 °C for 4 h. After the synthesis, the composite beads were subjected to the same post-synthesis treatment as ZB-W. ZIF-8 resin composite synthesized in methanol is denoted ZB-M-x, where the x is the concentration in mole of $Zn(NO_3)_2 \cdot 6H_2O$ solution used for Zn-exchange of initial resin beads.

Decontamination experiments

Methyl blue test: 10 mL methyl blue aqueous solutions with concentrations ranging from 5 to 250 mg L^{-1} was poured into 25 mL glass bottle containing 10.0 mg of adsorbent, i.e. ZIF-8 powder, Zn-exchanged resin beads and the ZB-W-1.5 composite, then agitate on a shaker (200 rpm) for 2 h. The supernatant was separate from the adsorbent and the remaining concentration of MB was determined by UV-Vis spectrophotometer. The same procedure was followed to evaluate the kinetics of MB adsorption on the three adsorbents.

After the adsorption test the ZB-W-1.5 was recovered by treatment with 1 M KBr solution in methanol. Typically, a 10 mL portion of KBr solution was added into a 25 mL glass bottle containing 10.0 mg of exhausted ZB-W-1.5. The mixture was shacked at room temperature for 1 day, and then the beads were separated, washed with methanol and dried to be reused. The recyclability test was repeated 10 times.

Oxytetracycline test: 10 mL oxytetracycline aqueous solutions with concentration from 5 to 250 mg L^{-1} was poured into 25 mL glass bottle containing 10.0 mg of adsorbent, i.e. ZIF-8 powder, Zn-exchanged resin beads and ZB-W-1.5 composite, then shacked with 200 rpm at room temperature for 2 h. The supernatant was separate from the adsorbent and the remaining concentration of OTC was determined by UV-Vis spectrophotometer. Absorption spectra at various concentrations of the MB and OTC solution were recorded to prepare the standard curves (Fig. S1 and S2, respectively). The adsorbed capacity q_e for MB and OTC were calculated by using the mass balance Equation: $q_e = (C_o - C_e) * V/M$, where C_o and C_e is the initial and the equilibrium concentration of solution [mg L^{-1}], V is the volume of solution [L], and M is the mass of adsorbent [g]. All experiments were repeated three times.

Characterization

Powder X-ray diffraction (PXRD) analysis was performed on a PANalytical B.V. Empyrean powder diffractometer at 40 kV and 40 mA using Cu Kα radiation (λ = 1.5418 Å) over the range of 2θ = 4.0 – 40.0° Two Theta. Thermogravimetric analysis (TGA) was performed using a SHIMADZU DTG-60 thermal analyzer system from 30 to 800 °C under air atmosphere at a heating rate of 10 °C min^{-1}. Before XRD and TGA analysis the microspheres were ground into powder in an agate mortar. A JEOL JSM6700 scanning electron microscope was used to study the morphology of the samples. Nitrogen adsorption analysis was performed with a Quantachrome Autosorb-IQ analyzer with ultra-high-purity nitrogen gas (99.999% purity). Prior to the analysis the samples were outgassed at 140 °C for 24 h. A SHIMADZU UV-2450 spectrophotometer was used to analyze the concentration of MB and OTC in water solutions.

The results of MB adsorption experiments were analyzed employing the Langmuir (1), Freundlich (2) and Temkin (3) model equations:

$$Ce/qe = 1/K_L\, q_{max} + Ce/q_{max} \quad (1)$$

$$\ln q\, e = \ln K_F + 1/n \ln C_e \quad (2)$$

$$q_e = RT/b \ln K_T + RT/b \ln C_e \quad (3)$$

where q_{max} denotes the maximal adsorption capacity and K_L, K_F and K_T represents these adsorption model constants respectively; and R is the universal gas constant (i.e., 8.314 J K^{-1} mol^{-1}); T is the temperature in Kelvin (K).

Results and discussion

ZIF-8 was successfully synthesized in both, water and methanol medium (Fig. 1). The synthesis experiments were performed in water and methanol medium after pre-treatment of the beads with 0.5, 1.0 and 1.5 M $Zn(NO_3)_2 \cdot 6H_2O$ water solutions. The purpose of the pre-treatment procedure is to obtain Zn-form of resin beads. Zinc is a building component of ZIF-8 and the preliminary Zn exchange favours the growth of molecular sieve material. The series of samples obtained in water (Fig. 1a) show higher crystallinity in respect to the counterparts obtained in methanol (Fig. 1b). The XRD study revealed also that the pre-treatment with $Zn(NO_3)_2 \cdot 6H_2O$ solution plays important role in the following crystallization step. Thus, the beads with highest X-ray crystallinity were obtained after using 1.5 M $Zn(NO_3)_2 \cdot 6H_2O$ solution. It should be noted that a small amount of unidentified phase was observed in the products synthesized in methanol (Fig. 1b).

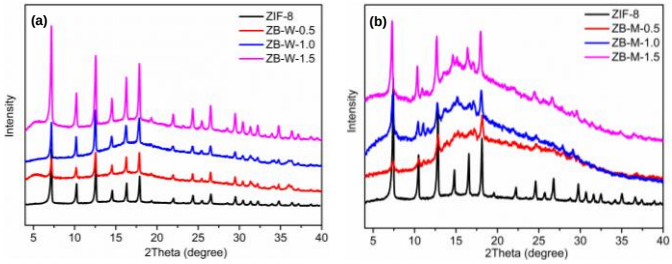

Fig. 1 Powder XRD patterns of the series of ZIF-8 - resin bead composites synthesized in water (a) and methanol (b) medium.

Parent and composite beads (ZB-W-1.5 and ZB-M-1.5) were studied by SEM (Fig. 2). The original shape and dimension of resin beads was maintained after the crystallization process. Parent cation exchange resin beads exhibit smooth external surface without any particles (Fig. 2a). The volume is built of polymer network without particular morphological features (Fig. 2d). The inspection of external surface and cross-sections of composite beads revealed some differences in the crystallization process in water and methanol medium. Both, external surface and pore volume of water synthesized beads contain ZIF-8 crystals (Fig. 2b, e). In contrast, only the external surface of the beads synthesized in methanol is covered with ZIF-8 (Fig. 2c), while no MOF particles are detected in the volume of the beads (Fig. 2f). The formation of ZIF-8 exclusively on the external surface of resin beads explains relatively low crystallinity of the composites obtained in methanol medium (Fig. 1b).

Combined XRD-SEM study showed that the water medium is more efficient in the synthesis of ZIF-8 resin composites. Therefore, remaining part of the study was performed on the ZB-W-1.5 sample, which showed highest crystallinity and uniform distribution of ZIF-8 in the volume of resin beads.

N_2 adsorption analysis was used to evaluate the porosity and textural properties of the initial cation exchange beads, ZB-W-1.5 and ZIF-8 powder samples synthesized under similar conditions (Fig. S3). The results of N_2 adsorption analysis are presented in Table 1. Macroporous cation exchange resin beads exhibit negligible micro- and mesopore volume. As known the macropore volume cannot be evaluated by nitrogen adsorption. After the synthesis, the beads showed a certain increase of the micro- and mesopore volume (Table 1). The specific surface area rose from 13 m^2 g^{-1} for the parent beads to 238 m^2 g^{-1} for the composite beads. This increase in specific surface area is obviously due to the incorporation of ZIF-8. ZIF-8 synthesized under similar conditions showed S_{BET} = 1332 m^2 g^{-1} and micropore volume of 0.53 cm^3 g^{-1}. The increase in mesopore volume is attributed to the textural porosity generated by the intergrown ZIF-8 deposited in the confined space of macroporous beads.

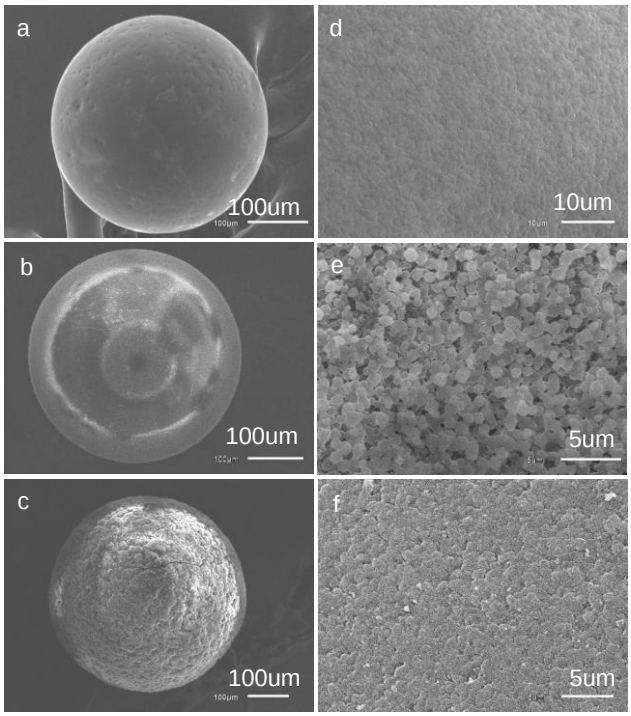

Fig. 2 Top and cross-section SEM micrographs of parent resin beads (a, d), ZB-W-1.5 (b, e) and ZB-M-1.5 (c, f) composites.

Table 1 Textural properties of resin beads, ZIF-8 and ZB-W-1.5 composite.

Materials	S_{BET}	Pore volume (cm^3 g^{-1})		
	m^2 g^{-1}	V_{mic}	V_{meso}	V_T
Resin beads	13	0.00	0.08	0.10
ZB-W-1.5	238	0.09	0.12	0.21
ZIF-8	1332	0.53	0.55	1.08

Thermal analysis was employed to evaluate the weight losses upon heating (Fig. 3). The total weight loss of Zn-exchanged initial resin beads was 88 %. About 25 wt. % was released between 25 and 400 °C and the rest between 400 and 730 °C. The low temperature

weight loss is attributed to water, NO_3^- groups and monomers loosely attached to the cross-linked polymer network. The combustion of polymer network is the origin of the second weight loss (ca. 63 %). Almost no weight loss in the temperature range 25-200 °C was observed for the ZIF-8. A weight drop of about 22 wt.% was recorded between 200 and 400 °C, followed by 60 wt. % loss between 400 and 600 °C. Composite beads showed the lowest total weight loss (63 wt. %), as about 5 wt. % were released between 25 and 400 °C. Lower weight loss in the low temperature range reveals the presence of ZIF-8 in the macropores of the resin beads. This volume is partially occupied by water and monomers in the case of parent Zn-exchanged beads. This conclusion is also supported by the lower total weight loss of ZIF-8 - resin composite.

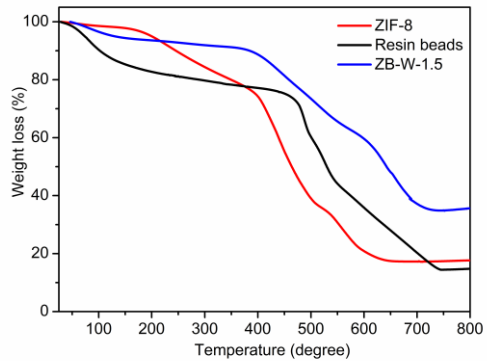

Fig. 3 Thermogravimetric analysis of ZIF-8, Zn-exchanged resin beads and ZB-W-1.5 composite.

The synthesized ZB-W-1.5 composite and the two basic components, i.e. resin beads and ZIF-8, were tested in decontamination of water containing hydrocarbon pollutants. The hydrophobic nature of ZIF-8 enables the interactions with hydrocarbons in water medium. Although the pore opening of ZIF-8 is relatively small the material was successfully used in the immobilization of hydrocarbons.[30] Charged polymer network of resin beads also exhibits adsorption properties owing to the electrostatic interactions between resin and charged species.

Fig. 4a shows MB adsorption curves of the three adsorbents for solutions with concentrations ranging between 5 and 250 mg L^{-1}. The duration of the experiment was 2 h. The adsorption capacities of all three adsorbents increased with the raise of MB concentration. Amongst them the cation exchange resin beads showed the lowest uptake. At low concentrations, up to 35 mg g^{-1}, ZB-W-1.5 and ZIF-8 powder exhibited similar behaviour. At higher concentrations the best performing material was the composite. The adsorbed amount as a function of the MB concentration was also studied (Fig. 4b). Almost no difference in the adsorption behaviour of cation exchange resin beads was observed. ZB-W-1.5 and ZIF-8 showed similar uptakes with an adsorption maximum at low concentration (*ca.* 25 mg L^{-1}). This result reveals that the adsorption ability of the composite is controlled by the ZIF-8 component. Yet, there is a certain synergy between cation exchange resin and ZIF-8 in the composite beads since the adsorbed amount is higher in the case of ZB-W-1.5.

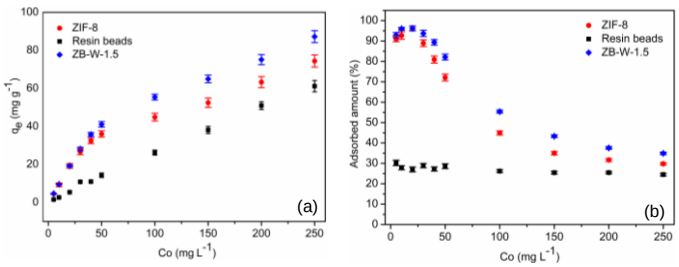

Fig. 4 Adsorption capacity (a) and adsorbed amount (b) of MB from solutions with different concentrations (adsorption time: 2 h, adsorption temperature: 25 °C, ZIF-8=0.2 g L^{-1}, resin beads=1 g L^{-1}, ZB-W-1.5=1 g L^{-1}).

MB adsorption isotherms were subjected to analysis employing Langmuir, Freundlich and Temkin models (Fig. S4). The data are summarized in Table 2. The analysis of obtained results shows that the Freundlich model exhibits the best correlation factors (R). Therefore, this model was further employed to study the adsorption kinetics. The adsorption behavior of MB and OTC is fairly similar; hence we anticipate similar adsorption mechanism for two molecules.

The kinetics of MB adsorption was studied employing a solution of 20 mg L^{-1} concentration in experiments with duration up to 200 min. In the first 50 min ZIF-8 shows the fastest uptake. We attribute this result to the fact that ZIF-8 sample is a powder of micron-sized crystals that is easily dispersed and thus rapidly reacts

Table 2 Adsorption isotherm model parameters derived from the Langmuir, Freundlich and Temkin model.

	Langmuir			Freundlich			Temkin		
Adsorbents	q_{max} (mg g^{-1})	K_L (L mg^{-1})	R_L^2	K_F (mg g^{-1}) (L $mg^{-1})^{1/n}$	n	R_F^2	K_T (J g^{-1})	b (J mol^{-1})	R_T^2
ZB-W-1.5	119.05	0.0093	0.978	2.02	1.40	0.958	0.159	32.49	0.962
Resin beads	434.78	0.0007	0.800	0.311	1.04	0.999	0.095	46.02	0.830
ZIF-8	92.59	0.0120	0.983	2.21	1.51	0.947	0.180	39.74	0.974

with the solution. The size of cation exchange resin beads is 300-400 µm comprising a hierarchical system of macro-, meso- and micropores. Consequently, complex diffusion phenomena control the uptake in the large composite beads. Nevertheless, after first 30 min the composite adsorbent showed higher MB uptake and after 200 min reached almost 90 % MB sequestration (Fig. 5). For the same period of time ZIF-8 and parent resin beads showed 80 and 40 % MB uptake, respectively. It is worth noting that the content of ZIF-8 in the composite is substantially lower than the pure ZIF-8 sample used as a reference. Nevertheless, the composite beads perform better showing the advantages of reported shaping procedure.

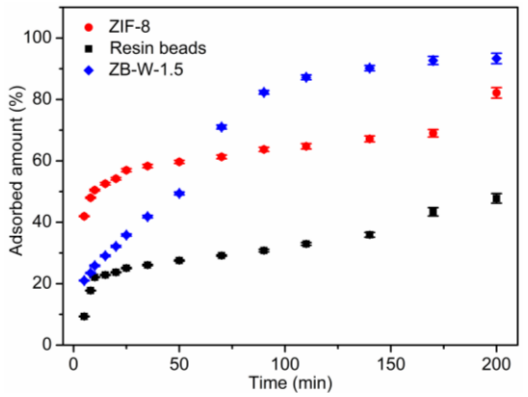

Fig. 5 Adsorbed amount of MB from 20 mg L^{-1} solution as a function of time (adsorption temperature: 25 °C, C*o*=20 mg L^{-1}, ZIF-8=0.2 g L^{-1}, resin beads=1 g L^{-1}, ZB-W-1.5=1 g L^{-1}).

To further analyze the adsorption kinetics pseudo-first-order equation and pseudo-second-order equation were employed: $\ln (q_e - q_t) = \ln q_e - k_1 t$ and $t/q_t = 1/k_2 q_e^2 + t/q_e$, where q_t (mg g^{-1}) and q_e (mg g^{-1}) are the adsorption capacities at any time and equilibrium, respectively, while k_1 (min^{-1}) and k_2 (g (mg^{-1} min^{-1})) represents the constant of pseudo-first-order rate and pseudo-second-order rate, respectively.[31] Table 3 shows the kinetic parameters derived from the linear regressions of the fitting results (Fig. S5). The R^2 values in the pseudo-second-order fitting are all close to 1 and higher than those in pseudo-first-order fitting.

Table 3 Kinetic parameters of MB adsorption on the three adsorbents at 25 ℃ for solution with concentration of 20 mg L^{-1}.

Adsorbents	Pseudo-first-order kinetic model			Pseudo-second-order kinetic model		
	q_e, mg g^{-1}	k_1, min^{-1}	R^2	q_e, mg g^{-1}	k_2, g mg^{-1} min^{-1}	R^2
ZB-W-1.5	21.6997	0.0548	0.9664	23.04	0.0010	0.9664
Resin beads	6.4237	0.0210	0.8597	9.35	0.0043	0.9463
ZIF-8	6.5358	0.0134	0.9152	13.91	0.0128	0.9981

The better correlation fittings indicate that the adsorption kinetic of MB on the composite adsorbent is well accorded with the pseudo-second-order model. Therefore, the adsorption behavior of the ZB-W-1.5 is controlled by surface phenomenon, i.e., the surface characteristics of the adsorbent.

Considering that different salts that influence the adsorption efficiency could be present in the contaminated water, we have studied the effect of NaCl on the adsorption of target molecules. NaCl was added to a MB solution (C*o*=20 mg L^{-1}) in concentrations ranging from 0 to 20,000 mg L^{-1}. Fig. 6 displays the removal rate as a function of NaCl concentration. As can be seen the adsorbed amount remained almost constant no matter the amount of NaCl. It is worth nothing that the adsorption behavior did not change even at very high concentration.

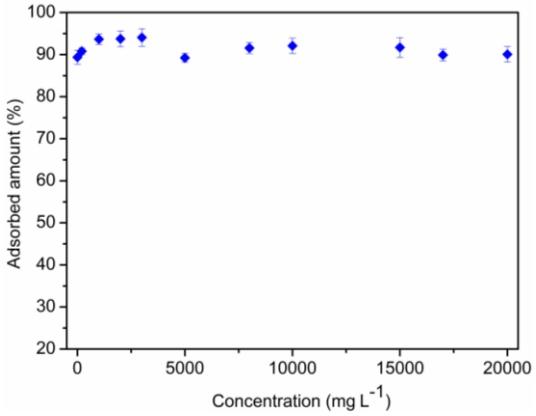

Fig. 6 Effect of NaCl concentration on the MB adsorption on ZB-W-1.5 (adsorption time: 2 h, adsorption temperature: 25 °C, C*o*=20 mg L^{-1}, ZB-W-1.5=1 g L^{-1}).

The effect of pH on adsorbent's behavior was also studied. The pH of our model MB solution (20 mg L^{-1}) was varied between pH 2 and 12 by adding HCl or NaOH. Fig. 7 shows the adsorption removal efficiency as a function of pH. At low pH (2-3), the removal efficiency decreased remarkably, indicating that the adsorption capacity will be profoundly hampered in an acidic environment. At pH values 4 and 5 the removal is 70 % and 90%, respectively and at

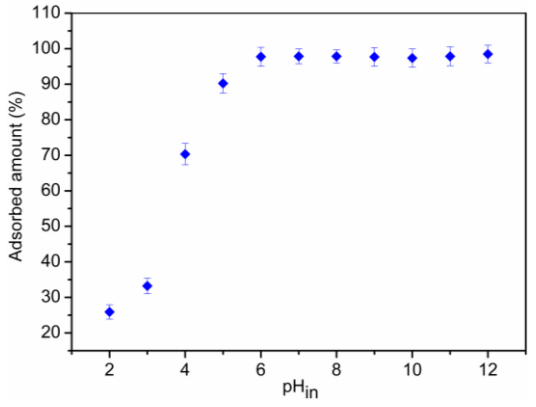

Fig. 7 Effect of pH on the MB adsorption ability of ZB-W-1.5 (adsorption time: 2 h, adsorption temperature: 25 °C, C*o*=20 mg L^{-1}, ZB-W-1.5=1 g L^{-1}).

pH over 6 it is closed to 100 %. These results show that the adsorbent can be used for the treatment of a great part of waste water sources.

No big changes in the ZIF-8 crystallinity after five and ten adsorption-desorption cycles were observed (Fig. S6). Noteworthy, the adsorption of MB can be followed with a naked eye by the colour of composite beads. As can be seen on the optical photographs, the colour of the beads changed from white to light purple and dark blue as a function of methyl blue concentration (Fig. S7).

The reusability of the composite adsorbent was also subjected to analysis. ZB-W-1.5 beads were treated in KBr solution to release the adsorbed dye and the adsorption experiment using 20 mg L^{-1} MB solution was repeated. After 10 adsorption-desorption cycles the composite still retains more than 80 % of its adsorption capacity (Fig. 8).

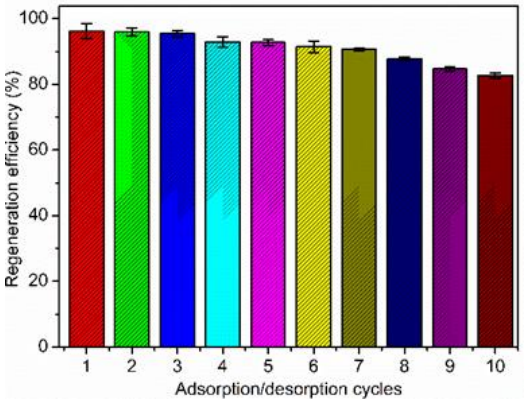

Fig. 8 Recyclability of ZB-W-1.5 composite adsorbent (adsorption time: 2 h, adsorption temperature: 25 °C, C*o*=20 mg L^{-1}, ZB-W-1.5=1 g L^{-1}).

The capability of studied adsorbents to immobilize oxytetracycline in water systems was studied using solutions with concentrations ranging between 5 and 250 mg L^{-1}. The adsorption time was 2 h. Fig. 9 summarizes collected adsorption data. The adsorption of OTC on the three adsorbents is similar with MB in term of adsorbed amounts (Fig. 4a). The two molecules are fairly similar in size, 15.7 Å and 13.95 Å for MB and OTC, respectively (Fig. S8). Both molecules are too big to be adsorbed in the micropore volume of ZIF-8. Thus, the adsorption is based on the p–p interactions between the aromatic rings of the pollutant and the imidazole linker.

The impact of molecule nature on the adsorbent behaviour, MB is an anionic dye and OTC is a neutral molecule, was studied in experiments with mixed solutions (Figure S5). A solution containing 20 mg L^{-1} MB and 20 mg L^{-1} OTC was employed and the adsorption time varied from 0 to 120 min (Fig.10). The set of experimental data shows a preferential MB adsorption in the first 35 min, which is almost completed in 35 min, while in the case of OTC the adsorption kinetics is much slower. We attribute this result of the negative nature of the anionic dye, which interacts with Zn cations

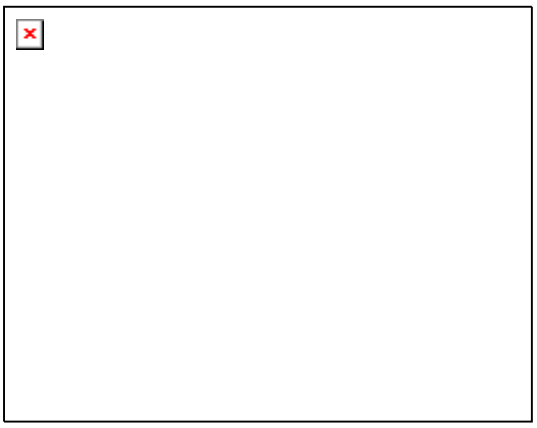

Fig. 9 Adsorption behaviour of ZIF-8, resin beads and ZB-W-1.5 in decontamination of OTC containing solutions of different concentrations (adsorption time: 2 h, adsorption temperature: 25 °C, ZIF-8=0.2 g L^{-1}, resin beads=1 g L^{-1}, ZB-W-1.5=1 g L^{-1}).

occupying the residual cation exchange sites in the resin beads. The result of this interaction is the preferential adsorption in the anionic dye in the beginning of the process, when dye concentration is relatively high.

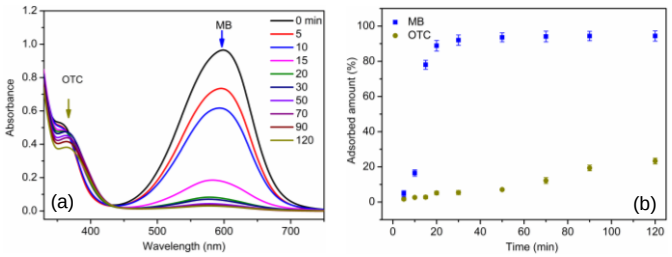

Fig. 10 UV–vis absorption spectra (a) and adsorbed amount (b) of mixed MB-OTC solution as a function of time (adsorption temperature: 25 °C, C*o*=20 mg L^{-1}, ZB-W-1.5=1 g L^{-1}).

A summary of the literature data reporting MB and OTC removal from water sources is presented in Table 4. Some of the adsorbents, namely carbon derivates, show higher adsorption capacity of MB and OTC in respect to our composite adsorbent. Nevertheless, the adsorbent capacity of the resin bead – ZIF-8 composite is fairly high. In addition, our material exhibits relatively high mechanical stability, define shape and size. In addition, the composite is easy to operate and recover and thus it can be used without additional processing.

The data of N_2 adsorption analysis and more precisely the micropore volume was used to evaluate the ZIF-8 content in the composite beads. The amount of ZIF-8 in the ZB-W-1.5 composite was found to be about 16 wt %. Although this estimation is not very precise it gives idea about the approximate content and allows discussing the decontamination performance of composite beads. ZIF-8 content is relatively low in the composite nevertheless it performs better in all adsorption experiments. Furthermore, the total capacity of composite beads is not a simple sum of the capacity of ZIF-8 and cation resin beads. For instance, the integral capacity of 80 % resin beads and 20 % ZIF-8 is still lower that the value recorded for the composite. This result unambiguously shows

that either ZIF-8 synthesized in the pores of the resin beads perform better than the crystal synthesized under conventional conditions or there is a synergetic effect between the two adsorbents. A possible explanation is that MOF crystals synthesized in the confined space of the beads are smaller in size and thus offer larger external surface area. In addition, the ZIF-8 crystals are deposited on the polymer network building the resin beads, which makes them highly accessible. Another factor that might influence the adsorption ability of the composite could be a possible modification of resin beads during the hydrothermal treatment in ZIF-8 yielding solution. These hypotheses, however, are difficult to be verified. Although the adsorption behaviour of composite beads is not fully elucidated, their excellent performance in sequestration of organic pollutant is not questionable.

Table 4 Literature overview and adsorption capacity of the adsorbents used for MB and OTC sequestration.

Adsorbent	Adsorbate	Adsorption capacity (mg g^{-1})	Ref.
GO grafted magnetic chitosan	MB	81	32
Fe_3O_4 /reduced graphene oxide	MB	75.15	33
Activated carbons	MB	250	34
Mn/MCM-41	MB	131.6	35
Exfoliated graphite/ZnO composites	MB	10.4	36
Organo-bentonite	MB	96.0	37
ZB-W-1.5	MB	88.2	Present work
Activated charcoal	OTC	408	38
Marine sediments	OTC	2.5	39
Amino-Fe (III) functionalized SBA-15	OTC	24.8	40
Polyaniline coated peanut shells	OTC	8.0	41
Carbon nanotubes	OTC	99.2	42
ZB-W-1.5	OTC	93.8	Present work

Conclusions

Cation exchange resin beads - ZIF-8 composites were prepared by hydrothermal synthesis. During the reaction ZIF-8 crystallized in the macropore space of the resin beads and thus an intimate mixture of two materials was obtained as the macro-morphological features of the resin beads were retained. The obtained composite was used for decontamination of water systems from hydrocarbons, as an anionic dye and an antibiotic were used as target pollutants. The results show a superior performance of the composite sorbent with respect to the parent resin beads and highly crystalline ZIF-8 powder.

The preparation approach developed in present study offers important advantages in respect to the previous art. Namely, the ion exchange resin bead carrier is robust and can withstand very harsh environment. In addition, the resin beads can be prepared with different size, available pore volume and surface functionality. The synthetic approach can be applied to different types of MOF, no matter of their chemical nature. Hence, this simple and efficient way for shaping MOFs is expected to open the route to practical uses of these promising molecular sieve materials.

Conflicts of interest

There are no conflicts to declare.

Acknowledgements

Q.F. and V.V. thank to the National Natural Science Foundation of China (21571079, 21621001, 21390394, 21571076 and 21571078) for the financial support. V.V. and Q.F acknowledge the support from Thousand Talents program (China).

Notes and references

1 T. B. Pushpa, J. Vijayaraghavan, S. J. S. Basha, V. Sekaran, K. Vijayaraghavan and J. Jegan, *Ecotoxicol. Environ. Saf.*, 2015, **118**, 177.
2 L. Shi, L. Hu, J. Zheng, M. Zhang and J. Xu, *J. Dispers. Sci. Technol.*, 2016, **37**, 1226.
3 K.Y. A. Lin and H. A. Chang, *Chemosphere*, 2015, **139**, 624.
4 M. Wawrzkiewicz, P. Bartczak and T. Jesionowski, *Int. J. Biol. Macromol.*, 2017, **99**, 754.
5 H. C. Su, Y. S. Liu, C. G. Pan, J. Chen, L. Y. He and G. G. Ying, *Sci. Total Environ.*, 2018, **616-617**, 453.
6 A. C. Singer, H. Shaw, V. Rhodes and A. Hart, *Front. Microbiol.*, 2016, **7**, 17.
7 P. Zhang, T. Wang, G. Qian D. Wu and R. L. Frost, *J. Colloid Interface Sci.*, 2014, **426**, 44.
8 J. Abdi, M. Vossoughi, N. M. Mahmoodi and I. Alemzadeh, *Ultrason Sonochem.*, 2017, **39**, 550.
9 G. Crini, *Bioresource Technol.*, 2006, **97**, 1061.
10 D. W. Breck, *Zeolite Molecular Sieves*, John Wiley & Sons, New York, 1973.
11 H. K. Chae, D. Y. Siberio-Pérez, J. Kim, Y. Go, M. Eddaoudi, A. J. Matzger, M. O'Keeffe and O. M. Yaghi, *Nature*, 2004, **427**, 523.
12 H. Furukawa, K. E. Cordova, M. O'Keeffe and O. M. Yaghi, *Science*, 2013, **341**, 6149.
13 L. Chen, R. Luque and Y. Li, *Chem. Soc. Rev.*, 2017, **46**, 4614.
14 G. Lu, S. Li, Z. Guo, O. K. Farha, B. G. Hauser, X. Qi, Y. Wang, X. Wang, S. Han, X. Liu, J. S. DuChene, H. Zhang, Q. Zhang, X. Chen, J. Ma, S. C. J. Loo, W. D. Wei, Y. Yang, J. T. Hupp and F. Huo, *Nature Chem.*, 2012, **4**, 310.
15 A. Huang, W. Dou and J. Caro, *J. Am. Chem. Soc.*, 2010, **132**, 15562.
16 D. Zacher, O. Shekhah, C. Wçll and R. A. Fischer, *Chem. Soc. Rev.*, 2009, **38**, 1418.
17 L. Hou, M. Zhou, X. Dong, L. Wang, Z. Xie, D. Dong and N. Zhang, *Chem. Eur. J.*, 2017, **23**, 13337.
18 H. Zhu, Q. Zhang and S. Zhu, *ACS Appl. Mater. Interfaces.*, 2016, **8**, 17395.
19 M. Matsumoto and T. Kitaoka, *Adv. Mater.*, 2016, **28**, 1765.

20 S. Aguado, J. Canivet and D. Farrusseng, *Chem. Commun.*, 2010, **46**, 7999.
21 L. D. O'Neill, H. Zhang and D. Bradshaw, *J. Mater. Chem.*, 2010, **20**, 5720.
22 T. T. Bui, N. D. Cuong, Y. S. Kim and H. Chun, *Mater. Lett.*, 2018, **212**, 69.
23 Z. Abbasi, E. Shamsaei, X. Fang, B. Ladewig and H. Wang, *J. Colloid Interface Sci.*, 2017, **493**, 150.
24 Y. Chen, X. Huang, S. Zhang, S. Li, S. Cao, X. Pei, J. Zhou, X. Feng and B. Wang, *J. Am. Chem. Soc.*, 2016, **138**, 10810.
25 L. Tosheva, B. Mihailova, V. Valtchev and J. Sterte, *Micropor. Mesopor. Mater.*, 2000, **39**, 91.
26 V. Valtchev, *J. Mater. Chem.*, 2002, **12**, 1914.
27 L. Tosheva, J. Parmentier, V. Valtchev, C. Vix-Guterl and J. Patarin, *Carbon*, 2005, **43**, 2474.
28 Y. Cao, Z. Pan, Q. Shi and J. Yu, *Int. J. Biol. Macromol.*, 2018, **114**, 392.
29 E. Korzeniewska and M. Harnisz, *Sci. Total Environ.*, 2018, **639**, 304.
30 Q. Yang, Q. Zhao, S. Ren, Z. Chen and H. Zheng, *Chem. Eng. J.*, 2017, **323**, 74.
31 Y. S. Ho and G. McKay, *Process Biochem.*, 1999, **34**, 451.
32 L. Fan, C. Luo, X. Li, F. Lu, H. Qiu and M. Sun, *J. Hazard Mater.*, 2012, **215-216**, 272.
33 P. K. Boruah, D. J. Borah, J. Handique, P. Sharma, P. Sengupta and M. R. Das, *J. Environ. Chem. Eng.,* 2015, **3**, 1974.
34 A. Zabaniotou, G. Stavropoulos and V. Skoulou, *Bioresour. Technol.*, 2008, **99**, 320.
35 Y. Shao, X. Wang, Y. Kang, Y. Shu, Q. Sun and L. Li, *J. Colloid Interface Sci.*, 2014, **429**, 25.
36 X. Yue, W. Duan, Y. Lu, F. Zhang and R. Zhang, *Bull. Mater. Sci*., 2011, **34**, 1569.
37 X. Hao, H. Liu, G. Zhang, Zou H, Y. Zhang, M. Zhou and Y. Gu, *Appl. Clay Sci.*, 2012, **55**, 177.
38 A. K. Alegakis, M. N. Tzatzarakis, A. M. Tsatsakis, I. G. Vlachonikolis and V. Liakou, *J. Environ. Sci. Health.*, 2000, **B35**, 559.
39 J. Li and H. Zhang, *Chemosphere*, 2016,**164**, 156.
40 Z. Zhang, H. Lan, H. Liu and J. Qu, *Colloids and Surfaces A: Physicochem. Eng. Aspects.*, 2015, **471**, 133.
41 F. Belaib, M. Azzedine, B. Boubeker and M. Abdeslam-Hassen, *Int. J. Hydrogen Energ.*, 2014, **39**, 1511.
42 L. Ji, W. Chen, L. Duan and D. Zhu, *Environ. Sci. Technol.*, 2009, **43**, 2322.